

On the stability of lateral self-mode locking in an injection laser

A.S. Logginov, K.I. Plisov

Abstract. The problem of coexistence and lateral self-mode locking in the resonator of an injection laser with a parabolically inhomogeneous permittivity is considered. The stability of the self-mode-locking process and factors causing its disturbance are studied. It is shown that the appearance of nonequidistant lateral modes due to the dependence of the refractive-index profile in a medium on the concentration of nonequilibrium carriers is the main cause of disturbing the self-mode-locking regime.

Keywords: injection lasers, emission dynamics, mode locking, numerical simulation.

1. Introduction

The electronic devices currently used in optical communication links operate at frequencies close to the limiting ones. This is a restraining factor on the way of further mastering the optical region in data transmission systems. Many of the existing electrical devices have no all-optical analogues. Therefore, studying the dynamic phenomena in active semiconductor media and structures is quite topical. The phenomenon of lateral self-mode locking in an injection laser diode (LD) can be useful in the development of devices with multistable radiation patterns and therefore employed for high-frequency synchronisation of spatially separated all-optical devices.

When an LD is developed, the lateral mode composition of its radiation is usually restricted to a single mode by narrowing its active region and thus preventing the excitation of higher-order lateral modes. The emission spectra of most of the modern LDs used in spectroscopy and information systems contain only a single zero-order lateral mode.

In earlier studies of LDs, the number of observed lateral modes was much larger, which was explained by the limited technological capabilities for manufacturing lasers. This feature allowed numerous dynamic effects to be observed [1, 2]. The understanding of these effects has led to the development of modern laser structures. For example, in

lasers, in the active region of which the refractive index became parabolically inhomogeneous during the growth of the $p-n$ junction, the emitting spot in the near field moved in some cases sinusoidally along the $p-n$ junction. This phenomenon could be observed thanks to the use of the electron–optical chronography method.

The first analytic studies of the laser emission dynamics for the laser active region with a parabolically inhomogeneous permittivity yielded the results that qualitatively coincided with the experimental data. In particular, it was shown theoretically for gas lasers with parabolic mirrors that, if several transverse modes, which are described in this case by Hermitian–Gaussian polynomials, exist simultaneously and have amplitudes distributed according to the Poisson law, sinusoidal scanning must appear [3].

Because the lateral resonator modes for a parabolic inhomogeneity of the permittivity in the active LD region are also described by Hermitian–Gaussian polynomials, the above theoretical analysis can be considered approximately valid for a semiconductor medium as well.

Semianalytic studies of simultaneous generation of several lateral Hermitian–Gaussian modes in an LD performed later on the basis of a numerical solution of rate equations yielded the data that agree well with the experimental data obtained earlier [4]. A discrete motion of the emitting spot in the near field was clearly demonstrated during the simultaneous generation of several lateral modes. Note that we are not aware of the works in which this process was observed in lasers with parabolic mirrors.

The fundamental possibility of the lateral mode locking was shown in [5] for an injection laser with a parabolic inhomogeneity of the permittivity in the active region. Below, we analyse the factors affecting the stability of mode locking. Its complete simulation is necessary for estimating the effect of the longitudinal distribution of the laser system on the mode-locking stability. When rate equations are used, this factor is neglected because of the averaging used in the derivation of these equations.

2. Mathematical model

Figure 1 shows a schematic drawing of the structure considered. It is assumed that a laser of length L and width w has an active region of width w_a and thickness d , through which a current of density J flows. The real part of the permittivity along the coordinate y has a parabolic profile.

To consider in detail the conditions for coexistence of lateral modes in the LD resonator, we adapted the standard

A.S. Logginov, K.I. Plisov Department of Physics, M.V. Lomonosov Moscow State University, Vorob'evy gory, 119992 Moscow, Russia; e-mail: as@osc.phys.msu.ru, k_plisov@mail.ru

Received 12 May 2004

Kvantovaya Elektronika 34 (9) 833–838 (2004)

Translated by A.S. Seferov

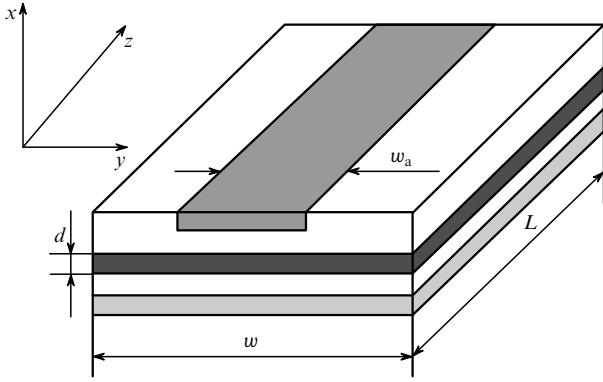


Figure 1. Scheme of the LD structure under study.

model [6] based on solving the diffusion equation for nonequilibrium carriers jointly with a parabolic equation of diffraction for the electromagnetic field; the latter was solved on the basis of the beam-propagation method (BPM). In this case, it is unnecessary to consider large diffraction angles, and the propagation of radiation can be regarded as paraxial with a high accuracy; i.e., the use of the BPM seems to be adequate. The mathematical adequacy of the Fourier transform along the lateral coordinate used in the BPM follows from the spatial limitation of the radiation field, which is determined by a strong waveguide effect caused by the amplification in the active medium.

As usual, we assume that the permittivity in the direction x (Fig. 1) in the active region undergoes a jump; as a result, a waveguide forms in this direction:

$$\varepsilon(x) = \begin{cases} \eta_a^2 & \text{inside the active region,} \\ \eta_p^2 & \text{in the emitter layers.} \end{cases} \quad (1)$$

The equation describing the propagation of radiation in the resonator has the form

$$\pm 2ik \frac{\partial \psi_\mu}{\partial z} + \frac{\partial^2 \psi_\mu}{\partial y^2} + k_0^2 \Gamma \Delta \varepsilon(y, z) \psi_\mu = 0, \quad (2)$$

where $k = k_0 \bar{\eta}$; $\bar{\eta}^2 = \Gamma \eta_a^2 + (1 - \Gamma) \eta_p^2$; ψ_μ is the electric field (index $\mu = f, b$ corresponds to two types of waves, forward and backward); $\Delta \varepsilon(y, z)$ is the contribution from all of the perturbations of the imaginary and real parts of the permittivity; k_0 is the wave number in a vacuum; $\bar{\eta}$ is the effective refractive index; and Γ is the optical confinement factor.

The initial condition for solving Eqn (2) is a small-amplitude electric field with a random spatial distribution, which must correspond to the spontaneous-recombination background. Equation (2) is homogeneous in functions ψ_μ ; therefore, the notion of ‘a small amplitude’ is uncertain for it and becomes meaningful only after the normalisation of the electric field for the diffusion equation for nonequilibrium-carriers is chosen:

$$\frac{\partial N}{\partial t} = \frac{J}{ed} + D_a \frac{\partial^2 N}{\partial y^2} - \frac{N}{\tau_{nr}} - \frac{\Gamma g(N)}{d \hbar \omega} (|\psi_f|^2 + |\psi_b|^2). \quad (3)$$

Here, N is the concentration of nonequilibrium carriers; e is the electron charge; D_a is the coefficient of ambipolar diffusion; τ_{nr} is the nonradiative recombination time;

$g(N) = aN - b$; a and b are the coefficient characterising the contribution from nonequilibrium carriers to the gain and the internal loss inherent to the material of the active medium; and ω is the optical radiation frequency.

The normalisation in Eqn (3) is chosen so that the integral of the square of the electric field over the lateral coordinate expresses the power in watts for all other parameters expressed in SI units.

The back effect of the concentration of inverted carriers on the electric field is taken into account by the coefficient $\Delta \varepsilon$ in Eqn (2):

$$\Delta \varepsilon = \frac{a \eta_a R N}{k_0} + i \left(\frac{\eta_a}{k_0} \right) (aN - b) - i \left(\frac{\eta_a}{k_0} \right) (1 - \Gamma) \frac{\alpha_p}{\Gamma}, \quad (4)$$

where R is the antiwaveguide parameter and α_p is the loss factor in passive regions.

Equation (2) was solved by the method of multiple forward and backward passage of radiation in the active medium in the resonator. After each round trip of the optical wave in the resonator, the inversion distribution resulting from burning out the inverted carriers by the field of the forward and backward waves was recalculated according to Eqn (3). Thus, the model actually takes into account the interaction of the forward and backward radiation waves through the nonlinearity of the active medium. If their interaction is ignored, it is easy to overlook the filamentation effect, which always manifests itself in an LD with a wide contact after a certain threshold current is exceeded. This inevitably leads to the decomposition of the initially specified mode structure in the nonperturbed resonator and excludes the existence of mode locking.

The substantial generality of the BPM, which is in essence a method for solving the parabolic diffraction equation, determines the subsequent efforts in revealing particular calculation results. These results are the spatio-temporal near-field radiation pattern and the time dependence in the concentration of inverted carriers.

One of the main features of the solution, which was obtained by the BPM, is the existence of a characteristic time scale – the round-trip transit for radiation in the resonator. This makes it impossible to observe several longitudinal modes, because we are constantly locked to a process having a width of the spectral window strictly equal to the spectral interval between adjacent longitudinal modes.

As follows from experiments performed earlier, the typical number of lateral modes associated with one longitudinal mode is no larger than ten and, for a favorable spectral gain profile, is independent of the order of the longitudinal mode. The principal factor determining this number is the ratio of the spectral intervals between the longitudinal and lateral modes. The number of lateral modes associated with one longitudinal mode depends on the size of the active region and the technologically preset permittivity profile.

Hence, after the chronogram of the near-field radiation is calculated, we can expect that approximately ten lateral modes will be selected. The mere generation of several lateral modes does not guarantee that their combining will result in a stable-in-time process of spatial scanning of the near- and far-field radiation. To initiate this process, two conditions should be satisfied: the amplitude of each mode should remain constant, and the intermode frequency

intervals should be equal.

The second requirement can be fulfilled, if an initial structure is created, in which the permittivity profile changes parabolically. However, the fact that this is valid for a passive resonator does not mean that it holds good for a laser, which is an essentially nonlinear system. For the initially equidistant modes, a change in the permittivity with time caused by the field-induced burning out of the inverse population may lead to a deviation of the mode spectrum from the equidistant one and thereby disturb the temporal stability of mode locking. The dependence of the imaginary part of the permittivity on the concentration of nonequilibrium carriers determines the time dependence of the amplitudes of the generated modes.

In order to assess the constancy of the mode amplitudes and verify the equidistance of the spectral intervals between them, each mode must be selected from the combined radiation-intensity distribution. For this purpose, the time-dependent near-field radiation spectrum must be calculated beginning with the moment when the transient process of reaching the steady-state lasing is completed.

The accuracy of calculating the spectral intermode interval obviously depends on the duration of the interval over which lasing is observed. As was mentioned above, the total width of the spectrum accessible for observation is determined by the round-trip transit time of radiation in the resonator. Thus, the error of measuring the spectral intermode interval is

$$\Delta\nu = \frac{1}{T} = \frac{c}{2Ln_{gr}N_{rt}}, \quad (5)$$

where T is the observation time of the process; c is the velocity of light; n_{gr} is the group refractive index; and N_{rt} is the number of round trips for radiation in the resonator after the achievement of steady-state lasing, during which the integral radiation pattern is recorded. Therefore, to estimate the intermode frequency with an accuracy of 10 MHz for a resonator 300- μm long, more than 10^4 round trips are required.

A typical calculated spectral-spatial radiation distribution shown in Fig. 2 clearly demonstrates a discrete structure of the excited lateral modes. The calculations show that

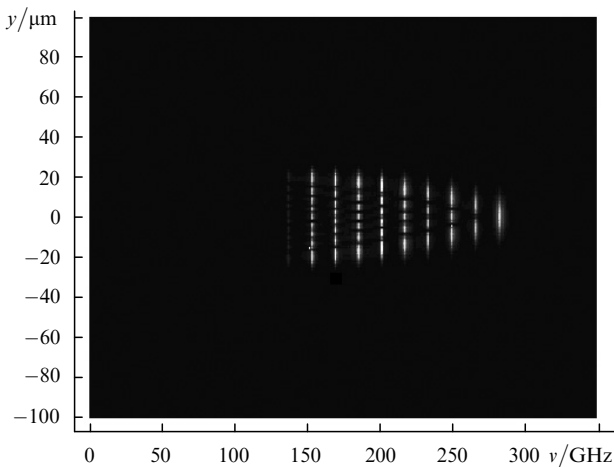


Figure 2. Calculated spectrum of multimode (in terms of lateral modes) lasing.

the modes are mutually orthogonal to within a high accuracy; therefore, by integrating the near-field chronogram over the found mode profiles, one can determine the time dependence of the amplitude of each mode. It is clear that we assume in this procedure that the spatial profile of each mode remains constant after the transient process is completed. Determining the amplitudes of modes from the near-field pattern during the transient process using the technique described above is senseless and may lead to unpredictable results.

The procedure of finding the amplitudes of modes from the near-field radiation distribution can formally be described as follows. If $E(y, t)$ is the calculated near-field radiation, then

$$S(y, \omega) = \int_{t_{th}}^{+\infty} E(y, t) \exp(i\omega t) dt, \quad (6)$$

$$A_n(t) = \int_{-w/2}^{+w/2} E(y, t) S_n^*(y) dy,$$

where $S_n(y) \equiv S(y, \omega_n)$ is the profile of the n th lateral mode; $n = 1, \dots, N$; N is the number of generated lateral modes; t_{th} is the duration of the transient process; $S(y, \omega)$ is the complete spectrum; and A_n is the amplitude of the n th mode.

3. Factors affecting the deviation of spectral intervals from equidistance

The spectrum of lateral modes may be nonequidistant due to two main factors: the contribution of nonequilibrium carriers to the permittivity and their burning out by the radiation field and due to the effect of the width of the active region on the mode spectrum.

A qualitative estimate of the effect a nonlinear contribution to the permittivity on the equidistance of spectral intervals between lateral modes can be obtained from the following considerations. The lateral modes of the electric field in the absence of inversion satisfy the equation:

$$B_m'' + \left[(\kappa_y)_m^2 - \frac{\omega_0^2}{c^2} \varepsilon_0 \frac{y^2}{s^2} \right] B_m = 0,$$

where s is the parabolic inhomogeneity parameter.

After an additional contribution (perturbation) appears in the permittivity due to the injected carriers, the eigenvalues corresponding to the perturbed permittivity also change. Assuming that the perturbations of the permittivity and eigenvalues are first-order infinitesimals, while the perturbations of eigenfunctions correspond to higher-order infinitesimals, the correction for the eigenvalues of modes can be written as

$$S_n'' + \left[-\frac{\omega_0^2}{c^2} (\varepsilon + \tilde{\varepsilon}) + \kappa_n^2 + \tilde{\kappa}_n^2 \right] S_n = 0, \quad (7)$$

where

$$\tilde{\kappa}_n^2(t) = \frac{\omega_0^2}{c^2} \int_{-w/2}^{w/2} S_n(y) \tilde{\varepsilon}(y, t) S_n^*(y) dy;$$

and $\tilde{\varepsilon}(y, t)$ is the permittivity perturbation depending on the

time and lateral coordinate. It is also assumed that functions $S_n(y)$ are normalised to unity and orthogonal.

Because the eigenvalues corresponding to nonperturbed eigenfunctions are equidistant, a nonequidistance in the resulting spectrum may appear only as a result of nonequidistant perturbations of the eigenvalues. If the difference of the permittivity perturbations for the n th and $(n+1)$ th adjacent modes is defined as

$$\Delta\varepsilon_n(t) = \int_{-w/2}^{w/2} S_n(y)\tilde{\varepsilon}(y,t)S_n^*(y)dy - \int_{-w/2}^{w/2} S_{n+1}(y)\tilde{\varepsilon}(y,t)S_{n+1}^*(y)dy \quad (8)$$

the nonequidistance of the spectral intervals adjacent to the n th and m th modes can be represented by the following sequence of relationships:

$$\begin{aligned} \frac{\omega_m}{c}\varepsilon_0^{1/2} &= k_0 + \frac{\kappa_m^2}{2k_0}, \\ \Delta\omega_m &= \frac{c}{2k_0\varepsilon_0}(\kappa_{m+1}^2 - \kappa_m^2), \\ \Delta\omega_{mm} &= \Delta\omega_m - \Delta\omega_n, \\ \Delta\omega_{mm}(t) &= \frac{c}{2k_0\varepsilon_0^{1/2}}\frac{\omega_0^2}{c^2}\operatorname{Re}[\Delta\varepsilon_m(t) - \Delta\varepsilon_n(t)], \\ \Delta v_{mm}(t) &= \frac{\omega_0}{4\pi\varepsilon_0}\operatorname{Re}[\Delta\varepsilon_m(t) - \Delta\varepsilon_n(t)], \end{aligned} \quad (9)$$

where ω_0 is the lasing frequency and ε_0 is the nonperturbed permittivity. The permittivity perturbation is generally a function of time and usually represents a function oscillating around its average value, which can be used as a qualitative estimate of the nonequidistance.

The width of the active region is the main parameter determining the number of modes that can exist within its limits. It also determines the amount of energy deposited into each mode. A change in the width of the active region cause a change in the ratio of the mode amplitudes. In some cases, this allows the control of the contrast of the interference pattern produced by the total radiation distribution.

In the direction of the y axis, the laser structure can be considered unbounded in the sense that the mode structure of the field in this direction is independent of the conditions at the physical boundaries of the resonator. In this case, the boundaries of the active region play the role of the boundary conditions, thus determining a limitation on the minimum width of this region: the eigenvalue corresponding to the resonator with a width equal to the width of the active region must be much smaller than the eigenvalues of the Hermitian–Gaussian polynomials, which appear when a parabolic permittivity profile is specified,

$$\left(\frac{\pi m}{w_a}\right)^2 \ll \frac{2k_0(m+1/2)}{s}. \quad (10)$$

Otherwise, the mode structure forms not due to the

parabolic inhomogeneity and an equidistant spectrum of lateral modes cannot be expected. The merit of the model based on using the BPM is that this circumstance is taken into account. This is a significant advantage over the model based on rate equations, which assumes that condition (10) is satisfied initially.

4. Results and discussion

When the dynamic processes occurring in an LD with locked lateral modes were simulated by the BPM, it was found at once that, in many cases, the simultaneous generation of lateral modes allows the observation of a pronounced-scanning regime only during a limited time interval. This regime is then disturbed and, after a certain time interval, recovers again (Fig. 3).

Figure 3a shows a chronogram of the near-field radiation over a quite long time interval. Four modes participate

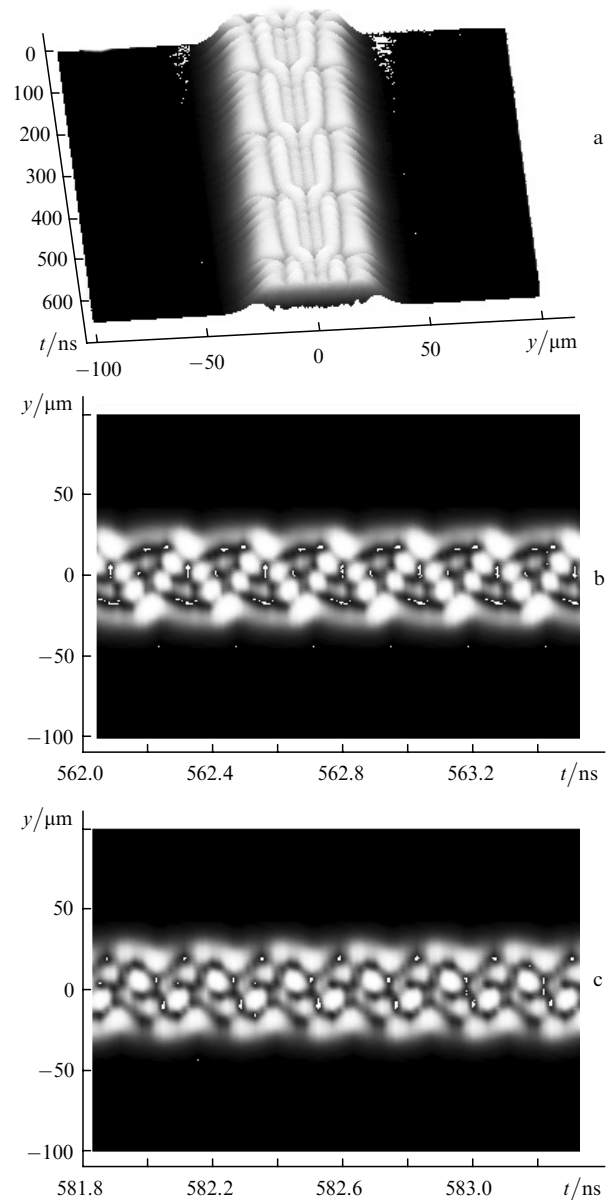


Figure 3. Calculated near-field chronograms for the generation of four modes: (a) time-integrated chronogram, (b) segment of sinusoidal scanning, and (c) segment without sinusoidal scanning.

in the mode-locking process. The spectral intermode interval that determines the scanning frequency is ~ 4.2 GHz. Pronounced sinusoidal scanning at this frequency is clearly seen in Fig. 3b. The grains observed in Fig. 3a represent a visualisation artifact. Since the time scale in Fig. 3a far exceeds that in Figs 3b and 3c, the scanning process in it is not resolved and we observe only a group of ‘continuously’ glowing regions that correspond to a fixed set of discrete positions of the emitting spot on the output mirror.

Similar phenomena were observed in earlier experiments (Fig. 4). This is certainly the encouraging agreement with the experiment. However, the main task is to obtain a stable scanning pattern. It follows from (10) that the eigenvalues of the modes in the active region increase much more rapidly than those of the modes of the waveguide formed by the parabolic permittivity profile; thus, an additional factor of deviation of the spectral intervals from equidistance appears for higher lateral modes. To eliminate the effect of the width of the active region on the nonequidistance of modes, the width was selected such that relationship (10) was valid for all the generated modes.

To verify the assertion that the remaining contribution to the nonequidistance is fully determined by the effect of nonequilibrium carriers, we performed numerical experiments, in which, first, the radiation power was constant and the antiwaveguide parameter of the laser structure was varied. After that, on the contrary, the antiwaveguide parameter was constant and the lasing power was varied proportionally to its previous changes. Such changes in these parameters ensured a constancy of their product, which contributed directly to the permittivity perturbation. A numerical calculation has shown that, within the accuracy provided by the calculation parameters, the deviation of the

spectral interval from equidistance is independent of what changes, either the radiation power or the antiwaveguide parameter, if their product remains constant.

The deviation of the intermode spectral intervals from equidistance was calculated directly from the near field calculated using (6). If the spatiotemporal dependence of the near-field radiation is known, we can calculate the time spectrum, which in turn determines the positions of modes and allows the calculation of the spectral intervals between them and, correspondingly, their deviation from equidistance. The calculation parameters are listed below.

Lasing wavelength $\lambda/\mu\text{m}$	0.82
Resonator length $L/\mu\text{m}$	300
Resonator width $w/\mu\text{m}$	200
Active strip width $w_a/\mu\text{m}$	75
Total thickness of the active layers $d_a/\mu\text{m}$	0.06
Reflectivity of the highly reflecting mirror R_1	1
Reflectivity of the output mirror R_2	0.9
Refractive index of the active region n_a	3.6
Refractive index of the passive regions n_p	3.3
Optical confinement factor Γ	0.1
Effective group refractive index n_{gr}	3.4
Antiwaveguide parameter R	1.8
Parabolic inhomogeneity factor s/cm	0.315
Coefficient a/cm^2	1.5×10^{-15}
Coefficient b/cm^{-1}	150
Nonresonant waveguide losses in passive regions α_p/cm^{-1}	10
Carrier lifetime τ_c/ns	1
Pump current density $J/\text{A cm}^{-2}$	170
Ambipolar diffusion coefficient $D_a/\text{cm}^2 \text{ s}^{-1}$	33
Number of round trips of radiation in the resonator.....	60000
Number of round trips of radiation in the resonator for which the time spectrum was calculated.....	55000

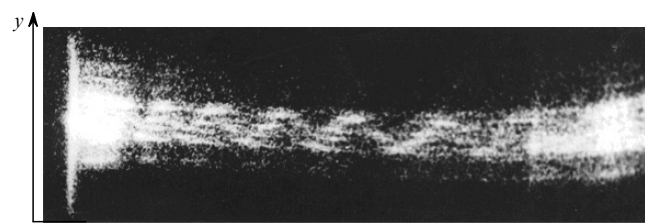


Figure 4. Experimental chronogram of the near-field radiation from a lateral-mode-locked laser. The scan duration is ~ 1 ns.

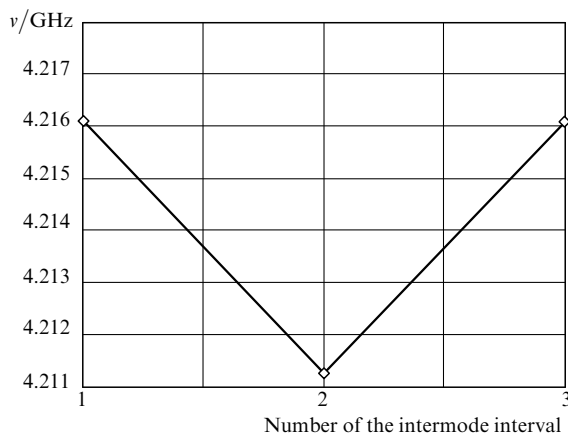


Figure 5. Calculated values of the intermode intervals.

The calculated spectral intervals are shown in Fig. 5, from which it follows that the deviation from equidistance is ~ 5 MHz. This value fully coincides with the period of disturbance of the mode-locking process (Fig. 3a).

Finally, it can be concluded that, if a mechanism for compensating for perturbations of equidistant spectral intervals is absent, the superposition of lateral modes simultaneously existing in an LD of planar geometry cannot lead to self-mode locking.

The self-action of the electric field through the nonlinear medium and the effect of the limited width of the active region result in a deviation of the spectral intervals from equidistance. This is displayed as a periodic disturbance and recovery of a harmonic radiation-scanning law. While the effect of the width of the active region on the mode composition can be overcome quite easily, the problem of compensating for the permittivity perturbations upon burning out the inversion requires further examination.

5. Conclusions

The beam-propagation method has been adapted and used to build a model that describes the simultaneous generation of lateral modes in an injection laser. It has been shown that by selecting appropriately the width of the active region, one can eliminate the effect of the width on the equidistance of lateral modes. Using the method developed, we have confirmed that the synchronous generation of lateral modes is violated due to the permittivity perturbation caused by burning out of the inversion by the electromagnetic field and by changes in the mode eigenvalues.

References

1. Vyshlov S.S., Ivanov L.P., Logginov A.S., Senatorov K.Ya. *Pis'ma Zh. Tekh. Fiz.*, **13**, 131 (1971).
2. Kurylev V.V., Logginov A.S., Senatorov K.Ya. *Pis'ma Zh. Tekh. Fiz.*, **8**, 317 (1968).
- [doi](#) 3. Auston D.H. *IEEE J. Quantum Electron.*, **4**, 420 (1968).
4. Logginov A.S., Plisov K.I. *Laser Phys.*, **14** (8), 1105 (2004).
- [doi](#) 5. Logginov A.S., Plisov K.I. *Kvantovaya Elektron.*, **32** (6), 553 (2002) [*Quantum Electron.*, **32** (6), 553 (2002)].
- [doi](#) 6. Agrawal G. *J. Appl. Phys.*, **56**, 3100 (1984).